Vol. 19, Sup. 1 (2020) 429-444
Revista Mexicana de Ingeniería Química

Sulfonated rim rubber used as a solid catalyst for the biodiesel production with oleic acid and optimized by Box-Behnken method

Hule de llanta sulfonada utilizada como catalizador sólido para la producción de biodiésel con ácido oleico y optimizada por el método box-Behnken

L.A. Sánchez-Olmos[1]*, M. Sánchez-Cárdenas[1], K. Sathish-Kumar[2], D.N. Tirado-González[3], F.J. Rodríguez-Valadez[4]

[1]*Direccion de Postgrado e Investigación, Universidad Politécnica de Aguascalientes, Calle Paseo San Gerardo 207, Aguascalientes, C.P. 20342, Ags, México.*
[2]*Instituto Tecnológico El Llano Aguascalientes (ITEL)/ Tecnológico Nacional de México (TecNM). Km 18 carr. Aguascalientes-San Luis Potosí, El Llano Ags., C.P. 20330, México.*
[3]*INIFAP/CENID agricultura familiar. Km8.5 carretera Ojuelos-Lagos de Moreno, Ojuelos, Jalisco, México. CP. 47540.*
[4]*Centro de Investigación y Desarrollo Tecnológico en Electroquímica S. C., Parque Tecnológico Querétaro, San Fandila Pedro Escobedo, C.P. 76703, Mexico*

Received: May 2, 2020; Accepted: June 24, 2020

Abstract

Esterification of oleic acid was carried out to obtain methyl esters at temperatures below the critical point of methanol in the presence of sulfonated carbon. That was obtained by pyrolysis from tire rubber and use as catalytic support after sulfonated. The sulfonated carbonaceous material in the laboratory was analyzed by spectroscopy and microscopic techniques: IR spectroscopy, X-ray diffractometry, programmed desorption at a temperature (ICTAC), X-ray photoelectron spectroscopy and scanning electron microscopy. The physicochemical properties of catalyst favor high performance in the production of biodiesel from oleic acid, are easily separated from the liquid mixture at the end of the reaction. At the temperature of 200 °C, with a reaction time of 20 min and a catalyst amount of 0.03% by weight, was the optimal experimental conditions for the esterification of oleic acid with methanol, giving a conversion of 97.9% of free fatty acids according to the response surface method. The Box-Behnken experiments were applied in order to evaluate the effects of the production parameters of biodiesel and find out the optimal conditions to obtain the maximum yield. Interestingly, stable catalytic activity in several reaction cycles was found.
Keywords: biodiesel production, solid acid catalyst, sulfonation treatment, Box-Behnken method, reaction cycles.

Resumen

La esterificación del ácido oleico se realizó para obtener ésteres metílicos a temperaturas inferiores al punto crítico del metanol en presencia de carbón sulfonado. Eso se obtuvo por pirolisis del hule de llanta y se usó como soporte catalítico después de la sulfonación. El material carbonoso sulfonado en el laboratorio se analizó mediante espectroscopia y técnicas microscópicas: espectroscopia IR, difractometria de rayos X, desorción programada a temperatura (ICTAC), espectroscopia de fotoelectrones de rayos X y microscopía electrónica de barrido. Las propiedades fisicoquímicas del catalizador favorecen un alto rendimiento en la producción de biodiesel a partir de ácido oleico, se separa fácilmente de la mezcla líquida al final de la reacción. A la temperatura de 200 ° C, con un tiempo de reacción de 20 min y una cantidad de catalizador de 0.03% en peso, fueron las condiciones experimentales óptimas para la esterificación del ácido oleico con metanol, dando una conversión del 97.9% de ácidos grasos libres según al método de superficie de respuesta. Los experimentos de Box-Behnken se aplicaron para evaluar los efectos de los parámetros de producción de biodiesel y descubrir las condiciones óptimas para obtener el máximo rendimiento. Curiosamente, se encontró actividad catalítica estable en varios ciclos de reacción.
Palabras clave: producción de biodiesel, catalizador ácido sólido, tratamiento de sulfonación, método de Box-Behnken, ciclos de reacción.

* *Corresponding author. E-mail*: luibandi_2000@hotmail.com
https://doi.org/10.24275/rmiq/Cat1625
ISSN:1665-2738, *issn-e*: 2395-8472

1 Introduction

Due to the gradual depletion of traditional fossil fuels and the increase in environmental pollution generated by these, alternative renewable energies are attracting more attention in recent years for industrial and transport purposes (Farobie *et al*., 2017). Biodiesel is a renewable biofuel that is almost compatible with commercial diesel engines and has strong advantages about diesel fuel, which includes better biodegradation, lower toxicity, and a lower emission profile (Lozano *et al*., 2013). Biodiesel is generally produced by the transesterification of triglycerides from vegetable oils or animal fats (Zhou *et al*., 2013) and also the esterification of free fatty acids (FFA) present in some used oils and virgin oils (Farobie *et al*., 2017). Biodiesel possesses physicochemical properties similar to those of fossil diesel, such as the value of cetane, lubricity, kinematic viscosity and flash point, and can be applied directly to the engine without mechanical modifications. Organic esters are of considerable economic interest due to their applications as solvents, extractants, plasticizers, lubricants, lubricating additives and even, in the case of some volatile esters, as aromatic compounds, in perfumes, cosmetics, and food reports (Wang *et al*., 2018). Oleic acid is present in natural oils and its esterification catalyzed by acid becomes a model reaction of biodiesel production (Mohammed *et al*., 2016; Sánchez-Cárdenas *et al*., 2016; Sánchez-Cárdenas *et al*., 2017). In recent literature reports the esterification of oleic acid with methanol. Further studied the homogeneous systems using mineral/acid-base catalysts have been well studied; thus recent innovations in this area tend to focus on increasing the yield of the product through an additional reaction treatment (Singh *et al*., 2018). The use of a basic liquid catalyst, with a high content of free fatty acids of low-cost raw materials, in most of the cases, leads to the formation of soaps, which considerably increases the separation costs of the product and separation of catalyst (Bing *et al*., 2019). Further, to eradicate this problem by utilization of the heterogeneous acid catalysts, (Cheryl-Low *et al*., 2015; Cea *et al*., 2019., Saravanan *et al*., 2015). The heterogeneous acid catalysts like sulfonated carbon are easily removed from the reaction mixture by filtration and can be recycled further by repeated processes (Long *et al*., 2014; Xie *et al*., 2014). Also, the loss of catalyst is avoided with reaction products, results in high purity. Besides, there is no soap formation in FFA (Baharudin *et al*., 2019). Considering the mesoporous carbon, whose surface is hydrophobic, manages to maintain unique porous properties (Zhang *et al*., 2018) and, therefore, the conversion of FFA into esters through sulfonated carbon. Hence esterification becomes a necessary pre-treatment of a catalyst with acids to obtain biodiesel, where FFA exists as in the case of spent vegetable oil (Sirisomboonchai *et al*., 2015; Li *et al*., 2019). The zeolites and ZrO are the most commonly used solid acid catalysts for the esterification of oleic acid with promising results. However, sulfonated carbon catalysts may have great potential as catalysts in the production of biodiesel for many reasons: the acidity is maintained in aqueous reactions having a large surface area with the homogeneity of porosity. In fewer cases, the sulfonated carbons used as catalysts showed better catalytic results than zeolites (Veiga *et al*., 2017; Paysepar *et al*., 2018). Besides, acid catalysts show the potential to direct both transesterification and esterification reactions in simultaneous reactions, allowing lower-cost raw materials to be processed (Chellappan *et al*., 2018; Chaveanghong *et al*., 2018). Due to above-mentioned reasons, the heterogeneous acid catalyst has the potential for the most economical biodiesel production process. Carbon materials have been extensively researched as functional materials for various proposals, including various applications in the petroleum and pharmaceutical industries, like adsorbents for water purification, electrode fabrication and catalyst supports for batteries and fuel cells (Noshadi *et al*., 2014; Shi *et al*., 2019). The use of these types of carbon-based solid acid catalysts, to direct esterification reactions in the production of biodiesel from oleic acid is acceptable for an economical process (Teo *et al*., 2014; Cannilla *et al*., 2018; Rechnia-Goracy *et al*., 2019). Conversion of waste to valuable product has a potential application in the sustainable environmental process. In this sense, our work has focused on the optimisation (reaction time, temperature and catalyst loading) of waste to energy conversion from the used tire as a solid acid heterogeneous catalyst for the effective conversion of oleic acid esterification to produce biodiesel. Further, demonstrated their sustainable re-utilization of the catalyst after several cycles.

2 Materials and methods

2.1 Materials

Oleic acid, methanol, sulfuric acid was obtained from SIGMA-ALDRICH. All the chemical products were analytical reactive grade and used as such.

2.2 Preparation of sulfonated carbon catalyst

The preparation of solid acid catalyst (CAS) began with a thermal pyrolysis process, where 10 g rubber tire was placed into a stainless steel micro-reactor at a temperature of 520 °C, with a heating ramp of 15 °C/min and an N2 flow of 30 mL/min for 2 hours. The sulfonation process was carried out on the carbonaceous material (CTE) obtained, where 20 g of CTE and 200 mL of H_2SO_4 were taken. The mixture was placed in a 1000 mL flask at 140 °C for 12 hours, then the suspension obtained was washed with hot deionized water at 80 °C until neutral pH and further filtered and dried at 120 °C for 24 hours in an oven.

2.3 Physicochemical characterization of the catalyst

The obtained CAS was subjected to different physical characterization techniques: X-ray diffraction (XRD) was performed with a Brucker diffractometer model D8, for scanning electron microscopy (SEM) a JEOL JSM-6300-S electronic microscope was used, X-ray analysis of energy dispersion (EDX) was performed with an EDAX acquisition system. Infrared spectroscopy (FTIR) was analyzed in a Thermo Scientific Nicolet iS10 model spectrophotometer. The pore size distribution and surface area of the solid carbonaceous acid catalyst were determined by the nitrogen desorption method with a piece of Qantachrome Autosorb-1C equipment. The Raman spectra were obtained by means of a JASCO NRS-5100 Micro-Raman dispersion spectrophotometer, which uses a laser diode with a wavelength of 532 nm and 30 mW of power (Elforlight G4-30; Nd: YAG) with 5 accumulations. Acid catalyst sites were analyzed by the standard titration technique (Sánchez-Olmos *et al.*, 2017).

Figure 1. Home-built reactor for oleic acid esterification reactions.

2.4 Esterification reaction

To obtain biodiesel from oleic acid, 60 mL of oleic acid was mixed with 142 mL of anhydrous methanol in a flask. These quantities remained constant in the work, later they were placed inside the homemade construction reactor as shown in Figure 1. The main variables involved are percentage by weight of carbonaceous catalyst% (W), temperature (T) and reaction time (M). For the esterification reaction of oleic acid, a stainless steel reactor (Figure 1) was used with different amounts of CAS at different temperatures and reaction times with a heating ramp of 20 °C/min.

The reaction time is recorded at the time when the reaction temperature reached the desired value. Once the desired reaction time had elapsed, the reactor was quickly cooled by placing it in a container with water at 20 °C, so that the reaction would not continue and to avoid undesired products derived from reversible reactions (Jia *et al.*, 2018). The remaining mixture was placed in a separating flask, the catalyst and glycerine were separated from the solution whereas the unreacted methanol was recovered by evaporation, and the catalyst was recovered by vacuum filtration. The biodiesel obtained was analyzed by GC gas chromatography and 1 mL was used for each esterification reaction in the GC to calculate the FAME content according to eq. 1(Mota *et al.*, 2019):

$$FAME\% = \frac{\sum A - A_{EI}}{A_{EI}} \times \frac{C_{EI} \times V_{EI}}{m} \times 100 \quad (1)$$

Table 1. Value range and coded levels of the independent variables.

Independent variables	Symbol	Coded levels		
		-1	0	1
Temperature, °C	T	170	200	230
Reaction time, min	M	10	20	30
Catalyst amount, wt.%	W	0.01	0.03	0.05

Where ΣA is the total peak area of the methyl ester in C_{14} to that in $C_{24:1}$; A_{EI} is the peak corresponding to methyl heptadecanoate; C_{EI} is the concentration of methyl heptadecanoate solution in mg/mL; V_{EI} is the volume of methyl heptadecanoate solution in mL, and M is the mass of sample in grams.

2.5 Box-Behnken experimental design

The process for obtaining biodiesel is influenced by multiple variables by which an experimental design to determine the effect of operational factors and their interactions was carried out. The factors evaluated were wt. % of carbonaceous catalyst (W), temperature (T) and reaction time (M). The range of values and coded levels of variables are shown in Table 1.

The Box-Behnken design is a type of response surface methodology (RSM) commonly used as an experimental design in engineering characterized to be represented as an independent quadratic design. These designs are rotatable and require three levels of each factor. In the optimization procedure, a Box-Behnken experiment design with 15 experiments was used to fit a polynomial model and predict the performance of methyl esters as a function of independent variables and their interactions. Therefore, a polynomial model was used to estimate the yield of methyl esters (Y) in biodiesel. Therefore, Eq. 2 shows the response of quadratic polynomials (Kumar *et al*., 2014) as follows:

$$Y = \beta_0 + \sum_{i=1}^{k} \beta_i X_i + \sum_{i=1}^{k} \beta_{ii} X_i^2 + \sum_{i=1, i<j}^{k-1} \sum_{i=1}^{k} \beta_{ij} X_i X_j \quad (2)$$

where Y is the predicted response value, β_0, β_i, β_{ii} and β_{ij} are the regression coefficients (β_0 is the intercept coefficient (offset), β_i is the linear effect term, β_{ii} is the quadratic effect term and β_{ij} is the term interaction effect, X_i and X_j are the independent uncoded variables and k is the total number of independent variables.

The software "Statgraphics" (Centurion XV, 2006, Stat Point Inc., USA) was used to obtain the regression models of the response surface data. The statistical analysis was carried out by means of an analysis of variance (ANOVA). This analysis includes Fisher's relation (F) and the coefficient of determination (R^2) measures the fit accuracy of the polynomial model (Lokman *et al*., 2016; Dejean *et al*., 2017).

3 Results and discussion

3.1 Chemical and physical characterization of a solid acid catalyst

Hood *et al*., 2017 reported the novel acid catalyst from waste-tire-derived carbon. The process begins with the carbon derived from used tires and then use of L-cysteine as the source sulfur for the functionalization of the carbon surface. Most of the sulfur atoms derived from cysteine molecules are covalently connected through the disulfide bond, while some of them may exist in the form of thiol. Disulfide bonds can be efficiently reduced with dithiothreitol (DTT) under basic conditions (pH> 7) to generate thiols, which are then oxidized with H_2O_2 to generate sulfonic acid groups. Another batch of an experiment used carbon derived from sulfonated fuel waste tires by immersing it in concentrated sulfuric acid at 150 ° C for 15 hr with vigorous stirring and then washing with large amounts of deionized water. Likewise, the oxygen contents are 60% and 110%, respectively, concerning the original carbon. In the cysteine based procedure to modify the used tire carbon exhibited the greater sulfonation which did not adversely affect on a carbon support.

Mesoporous/microporous carbon derived from usted tires through direct ultrasound and dehydration procedures, which leads to intimate contact between ferric sulfate and carbon support. Amendment of the amount of ferric sulfate in the reaction might change in pores of the catalyst, where 10 wt% of ferric sulfate produced catalysts with improved kinetics towards FFA esterification compared to another sulfate ferric load these catalysts efficiently raw materials that are rich in FFA content to FAMEs, even in the presence of

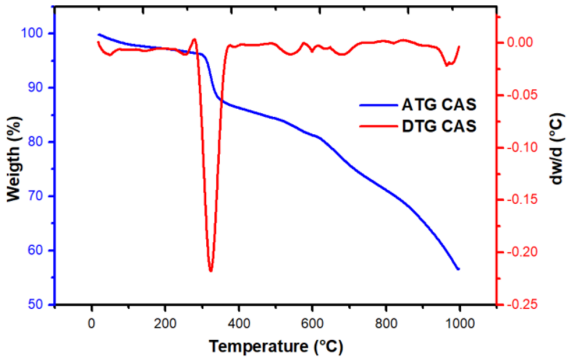

Figure 2. Thermogravimetric analysis of sulfonated char (CAS).

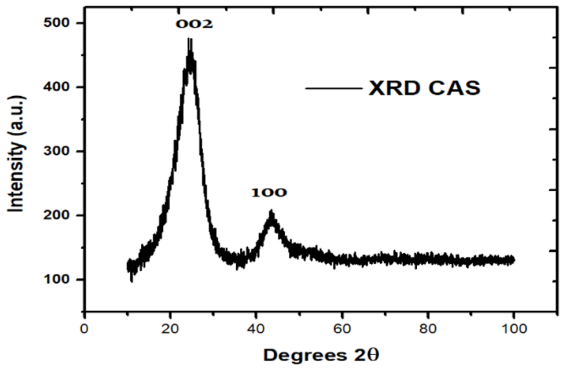

Figure 3. XRD pattern of the sulfonated carbon-based material.

decreased methanol problems, increased triglyceride concentrations, or relatively high water content (Hood *et al*., 2018). We obtained the carbon from the used tire at the minimum temperature and time (520 C and 2 hrs). This could reduce the use of energy consumption to produce carbon from the used tire. The quantification of the acid density in the CAS was carried out by the acid-base titration method giving a density of acidic groups of 2.82 mmol/g, which are strongly anchored in the carbon layer (Sánchez-Olmos *et al*. 2017). Therefore, CAS was suitable as an acid catalyst to produce biodiesel from oleic acid. Figure 2. shows the thermal stability of CAS by ICTAC under nitrogen flow, in which two important transition zones are exhibited. The first region at 36 to 120 ° C, which has a mass loss of about 5.1% by weight attributed to the release of physically bound water and probably a loss of -OH groups. The second transition at 121-300 ° C is attributed to the decomposition of the remaining organic groups due to the presence and stability of the covalent bond between the sulfonic site (-SO_3H) and the carbon surface. Above 520 ° C, the functional acid group (COOH) is removed (Tang *et al*., 2019). An important third stage appears in a range of high temperatures ranging from 720 to 960 °C due to the presence and stability of the covalent bond between the sulfonic site (-SO_3H) and the carbon surface (Douzandegi *et al*., 2019). These interesting results suggest that sulphonic groups reside predominantly within the micropores of the porous carbon instead of surfaces and walls of the macropores.

The X-ray diffraction pattern of the carbon sample is represented in Figure 3. The sample exhibited high background intensity, which indicates that the carbon contained a proportion of highly disordered materials in the form of amorphous carbon (Purova *et al*., 2015). The diffractogram shows the presence of an asymmetric band peak (002) around 25.5°, which indicates the separation of the aromatic ring layer, in addition, the carbons also include other structures such as graphite like. The second peak (plane 100) can be attributed to disordered carbon. These observations suggest that the carbon have an intermediate structure between the graphite and amorphous state called turbostratic structure (Liu *et al*., 2015; Saravanan *et al*., 2016).

The surface area and porosity presented in the CAS was 98.0 m^2/g. As a result of this, the CAS is a mesoporous catalyst (Guan *et al*., 2017). In Figure 4., the SEM image of the CAS is showed. It consists of particles of different sizes and irregular diameters of 3-40 μm. However, the large aggregate particles could be formed as a consequence of the agglomeration generated during sulfonation treatment by solid-state reactions.

To determine the percentage by weight and the atomic percentage, an analysis of samples by EDX was made to the CAS. Figure 4. is an SEM scan of the sulfonated carbon powder and the EDX chemical analysis obtained. The elemental analysis shows that carbon (C) and oxygen (O) are indeed present in this sample, the EDX analysis confirmed the presence of a significant amount of sulfur (S).

The presence of other minor elements such as Zn, Al, Si, Ca and Fe in CAS, due to the tire components (Calcite and Zincite). These compounds are used as an improved filling for a better tire formation. However, the presence of these elements in inert conditions, since it did not affect the biodiesel conversion (Yuvaraj *et al*., 2018). The value of the minimum emission voltage of Sulfer was approximately 2.36 keV. This analysis showed the amount of C and S in the CAS shown in Table 2. Where 3.21 wt. % of S is

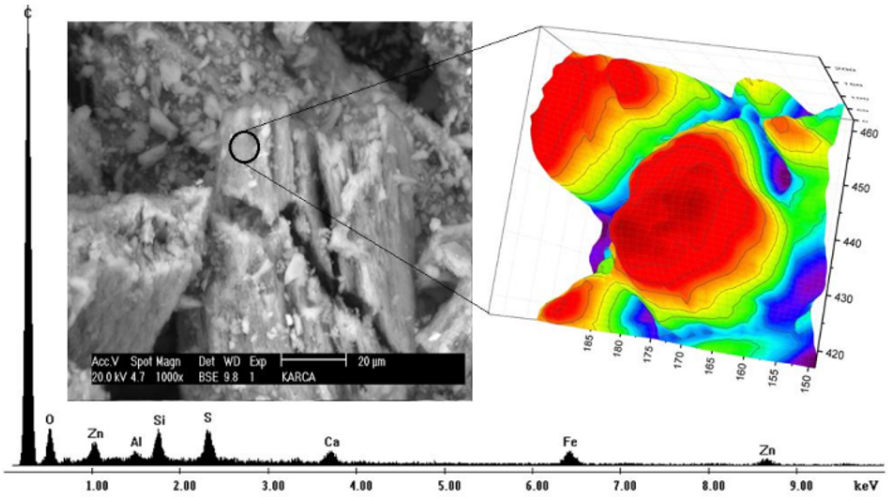

Figure 4. SEM image of CAS and EDX analysis.

Table 2. Elemental composition of CAS.

Sample	**C**		**O**		**S**	
	wt.%	at.%	wt.%	at.%	wt.%	at.%
CAS	91.79	94.94	3.89	2.98	3.21	1.12

at.%: Atomic composition in percentage

observed, showing a supported sulfur content after the sulphonation process. From the chemical composition of CAS, it can be concluded that for every 200 atoms of C, there are approximately 3 and 6 atoms of S and O on the catalyst surface, respectively.

The IR spectrum for CAS (Figure 5.) shows a first peak located at 617 cm^{-1} with a weak intensity corresponding to the SO link according to data reported in the literature (Fadhil *et al*., 2016; Efimov *et al*., 2018). A peak of vibration at 726 cm^{-1} corresponds to the aromatic fraction with average intensity. A signal at 1254 cm^{-1} with a weak intensity corresponds to the aromatic ring C-C. One of the most important peaks of IR is positioned at 1074 cm^{-1}, which has a strong intensity assigned to acid groups -SO_3H and represented by the symmetric vibration of O=S=O (Guan *et al*., 2017; Araujo *et al* 2019). Other IR peaks are observed at 1447 cm^{-1} and 1717 cm^{-1} with strong and medium intensities corresponding to the aromatic carbon (C=C) and the conjugated functional group C=O, respectively (Shukla *et al*., 2016; Sánchez-Olmos *et al*., 2019). The -CH_2- and -CH_3 groups (sp^3 carbon) - 2909 cm^{-1}, the vibrational frequency would associate with the inelastic neutron spectroscopy (INS) vibrational stretching modes of C-H, would represent at the higher range (~380 meV) as reported by Hood *et al*., 2019.

The Raman spectroscopy was applied to the CAS sample to analyze the structural integrity of carbon. Two bands are considered to be very important, G and D1 bands. Band G (1586 cm^{-1}) shows the presence of 2D graphene in a hexagonal network caused by the vibration of sp^2 carbon atoms (Figure 6.). The D1 band (1362.5 cm^{-1}) indicates defects and disordered carbon structures related to vibrations of sp^3 carbon atoms. The intensity of the G band in CAS is slightly higher than that of the D1 band; this indicates the presence of fewer defects and greater graphite character than in the original charcoal. The lowest D1/G ratio in the CAS material is maintained despite the incorporation of sulfur heteroatoms (carbons sp^3 formation) during sulfonated treatment (Medina-Valtierra *et al*., 2017). Therefore, we can conclude that treatment with sulfuric acid not only promotes the bonding of sulfonyl groups on the surface of carbon and also eliminates impurities on the carbon. The intensity of the D band is slightly higher than the G band. From the D/G ration exhibited the 0.94 value could represent the disorder origination in the CAS.

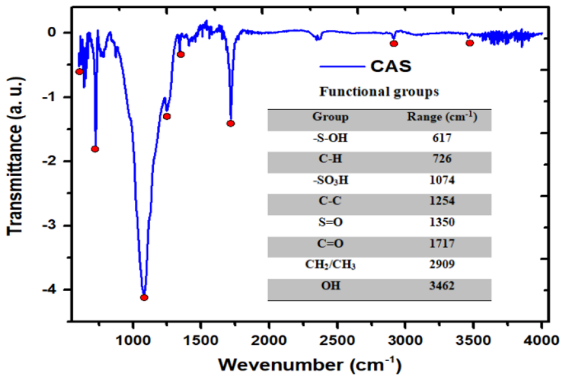

Figure 5. FTIR spectra of CAS.

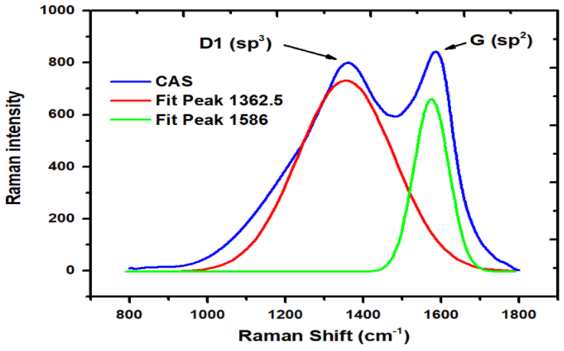

Figure 6. Raman spectra of sulfonated carbon (CAS).

3.2 *Effects of reaction parameters*

The amount of W catalyst, the T temperature and the M reaction time in biodiesel production are crucial performance parameters. Deactivation of the catalyst occurred as a result of contact between the used vegetable oil and methanol in the reaction mixture (Li *et al*., 2019). However, the molar ratio of methanol-oleic acid is one of the main parameters that affect the yield of biodiesel during the esterification reaction. Stoichiometrically, one mole of alcohol is required to esterify one mole of oleic acid and obtain one mole of alkyl esters and one mole of water. Since the esterification of oleic acid is a reversible reaction, an excess of alcohol is required to shift the equilibrium towards the formation of biodiesel (Choi *et al*., 2019).

3.3 *Experimental design*

In order to verify the model, 15 runs were carried out to obtain the response values as listed in Table 3. The agreement between real and predicted values was evaluated by the coefficient of determination (R^2). Ideally, the complete agreement between experimental and predicted values will be reached when R^2 is 1.

After performing the experiments defined by the Box-Behnken method in the equipment designed for this aim, Table 4. shows the results obtained in the tests carried out. Performance data were calculated from GC with equation 3 as follows (Dhawane *et al*., 2016; Veljković *et al*., 2018):

Table 3. Box-Behnken design for experiments with three factors and three levels.

Test	Reaction time, min	Temperature, °C	Catalyst, g
1	10	230	0.03
2	10	200	0.01
3	10	170	0.03
4	10	200	0.05
5	20	200	0.03
6	20	200	0.03
7	20	170	0.05
8	20	170	0.01
9	20	230	0.01
10	20	230	0.05
11	20	200	0.03
12	30	200	0.05
13	30	170	0.03
14	30	200	0.01
15	30	230	0.03

Table 4. Results obtained from the development of experimental tests.

Test	**Reaction temperature, °C**	**Catalyst, wt.%**	**Reaction time, min**	**Experimental yield, mol%**	**Theoretical yield, mol%**
1	-1	1	0	71.14	73
2	-1	0	-1	73.17	72.91
3	-1	-1	0	80.52	79.48
4	-1	0	1	78.29	77.72
5	0	0	0	97.9	97.9
6	0	0	0	97.9	97.9
7	0	-1	1	91.77	93.37
8	0	-1	-1	81.79	83.09
9	0	1	-1	82.7	81.1
10	0	1	1	87	85.7
11	0	0	0	97.9	97.9
12	1	0	1	92.88	93.14
13	1	-1	0	92.48	90.62
14	1	0	-1	82.49	83.06
15	1	1	0	86.4	87.44

Table 5. Values of statistical coefficients of yield and their statistical significance (F-ratio and p-value).

Source	Coefficient	B	F-ratio	p-value	Value
	β_0	95.15			95.15
A:M	β_1	326.785	88.9	0.0002	326.785
B:T	β_2	46.6578	12.69	0.0162	46.6578
C:W	β_3	110.931	30.18	0.0027	110.931
AA	β_{11}	346.425	94.25	0.0002	346.425
AB	β_{12}	2.7225	0.74	0.4288	2.7225
AC	β_{13}	6.94322	1.89	0.2277	6.94322
BB	β_{22}	114.914	31.26	0.0025	114.914
BC	β_{23}	8.0656	2.19	0.1986	8.0656
CC	β_{33}	156.3	42.52	0.0013	156.3

$$\text{Yield of FAME (\%)} = \frac{\text{Weight of biodiesel produced X FAME content (wt.\%)}}{\text{Weight of oil sample}} \quad (3)$$

The yield of oleic acid to methyl esters is in the range of 73.17% to 97.9%. The results indicated a good fit in the model and significant values of coefficients and their interactions are shown in Table 5.

We obtained a second-order polynomial equation (Equation 4) that manages to express a relationship between the response and variables:

$$Y = 97.9 + 6.39125 \times M - 2.415 \times T + 3.72375 \times W - 9.68625 \times M^2 + 0.825 \times M \times T + 1.3175 \times M \times W - 5.57875 \times T^2 - 1.42 \times T \times W - 6.50625 \times W^2 \quad (4)$$

An analysis of variance (ANOVA) was used to estimate the level of significance. The F-value of the model is 30.18 and the corresponding value of p is <0.0001. This implies that the model is significant. The possibility of 0.01% that the model is not significant could be attributed to noise.

In this case, six effects have a p-value less than 0.05, i.e., $\beta_1, \beta_2, \beta_3, \beta_{11}, \beta_{22}, \beta_{33}$ are those that showed significant effects. The results of the p-value greater than 0.1 for the terms β_{12}, β_{13} and β_{23} indicate that they are not significant. In addition, each term in the model was also evaluated to determine the significant impact of the p-value less than 0.0552.

In Table 5, it is shown that there was no significant difference between the experimental data and the

prediction of results. In this study, the value of R^2 was 98.27, which means that less than 2.0 % of the total variations do not fit into the model, that the mathematical model is adequate to cover more than 98.0 % of the total variations.

The closer the value of R^2 to one, the better the empirical models compared to the experimental data. On the other hand, the lower the value of R^2, the lower the relevance of the dependent variables in the model and their ability to explain the behavior of the variations (Jiang *et al*., 2013). In this study, the value of R^2 and the adjusted value of R^2 were 98.2714 and 95.1599, respectively, which means that predicted and experimental efficiencies are similar to a large extent. Table 5. presents a comparison between the predicted and actual values of the response and confirmed that experimental results show compliance with the predicted values (Medina-Valtierra *et al*., 2017). Stated that the coefficients of determination, R^2 and R^2 adjusted must be at least 0.80 for an adjustment of a preferable and approximate model are the most appropriate. Table 6. shows the combination of factor levels, with which the maximum biodiesel yield of 98.94% is obtained in the studied region. From these statistical studies, it is implied that the model is suitable for predicting oleic acid yields percentages as a function of the variables investigated. Ferreira *et al*., 2020 reported the catalytic activities in the esterification reaction of oleic acid (OA) with octanol (OcA) showed 91% of yield, are carried out under an inert atmosphere at 90 ° C using a catalyst / oleic acid ratio of 4.0% by weight and stirring at 500 rpm for 6h. Our reactor disegn exhibited the ideal yield of 98.9% under the less loading amount of catalyst and reduces the reaction time. This would be beneficial for the minimum energy conversion of Biodiesel production.

As shown in Figure 7, the higher conversion rate of the FFA increased the biodiesel yield as a function of temperature and catalyst. In other words, increasing the temperature shows that the biodiesel yield increases to 87.87% at 200 °C because the esterification reaction is endothermic in nature (Fraile *et al*., 2015). This can be attributed to the accelerated activation of the carboxyl group of the FFA at high temperature, making it available for nucleophilic attack by hydroxyl groups of alcohol (CH_3OH). The activation of FFA is difficult to be carried out due to the steric hindrance of its long alkyl chains and carbonyl groups. To enhance the nucleophilic attack of methanol in the FFA, the relatively high reaction temperature is needed to activate the carbonyl group (Sangar *et al*., 2019).

Table 6. Optimal conditions for maximizing the biodiesel yield.

Factor	Value
T, °C	198.1
M, min	23.5
W, wt.%	0.03464

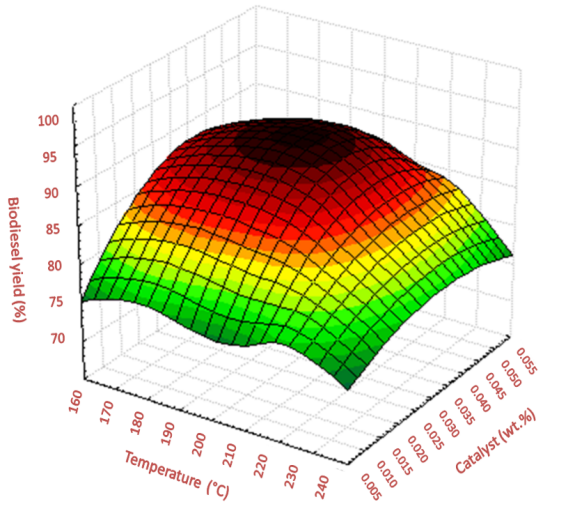

Figure 7. 3D response surface model for biodiesel performance as a function of reaction temperature and amount of catalyst.

This is because intrinsic rate constants are strong functions of temperature. Therefore, the high temperature promotes the rate of diffusion, since the reactants are more miscible (Jiang *et al*., 2013). This allows a higher reaction rate increasing the conversion and yield keeping constant the catalyst activity (Gao *et al*., 2015; Ning *et al*., 2017). When reaching the maximum temperature of reaction at 230 °C the yield of biodiesel is diminished, which can be attributed to the methanol polarity, therefore, the concentration of methoxide species in the reaction mixture decreases (Zhou *et al*., 2016) and as a result, the catalyst surface acidity is reduced while acidity value increases in biodiesel (Santos *et al*., 2015; Dhawane *et al*., 2018).

Figure 8. shows the biodiesel yield as a function of the reaction time and temperature. The production of FAME increases gradually with the increase in time, reaching a value that exceeds 97% at 23.43 min. The low production of biodiesel in a reaction time of the low level is attributed to the mass transfer effect (oleic acid-methanol-catalyst). Miscibility of oleic acid and methanol leads to diffusion limitations by reducing the reaction rate as time increases (Kurniawan *et al*., 2017). After reaching equilibrium, according to the Le

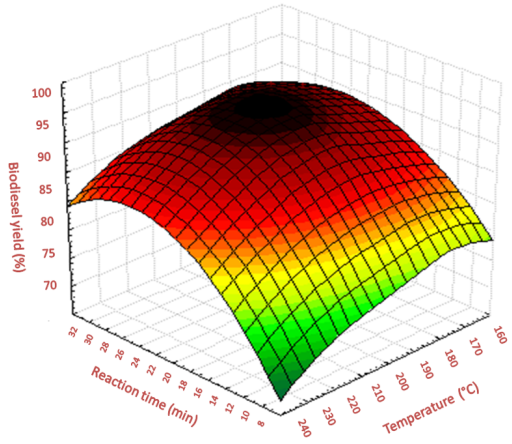

Figure 8. 3D response surface model for biodiesel performance as a function of reaction temperature and reaction time.

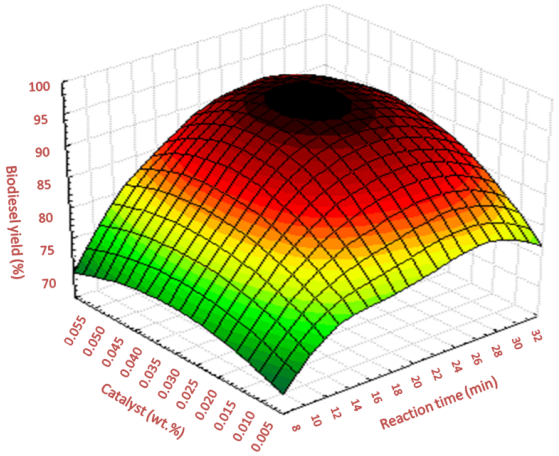

Figure 9. 3D response surface model for biodiesel performance based on the catalyst amount and reaction time.

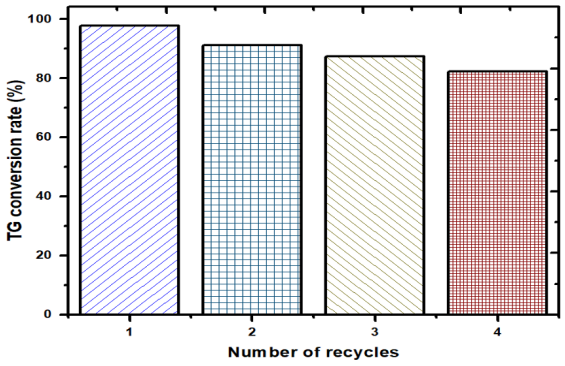

Figure 10. Capacity to reuse the CAS catalyst in reaction cycles of biodiesel conversion.

Chatelier principle, inverse reactions may occur and diminishing the biodiesel yield (Atadashi *et al*., 2012; Pisarello *et al*., 2018). On the other hand, the increase in temperature could lead to high conversion rates of FFA within certain limits. However, the maximum temperature would lead to a decrease in the FFA conversion rate.

Figure 9. shows the interaction between reaction time and catalyst with respect to the biodiesel yield. The active component of the catalyst is the sulphonic acid group (-SO_3H). It is evident that increasing the catalyst amount increases in the FAME yield. The sulfonic acid groups are found mainly on the porous surface of coal and being accessible to reactants to proceed for reacting (Hosseini *et al*., 2019).

An increase of biodiesel yield from 86 wt.% to 96 wt.% was obtained when varying the catalyst amount from 1 wt.% to 3 wt.%. This behavior can be attributed to the number of active sites available for the surface reaction and the mass transfer rate (Sarno *et al*., 2018). However, it was observed that a higher concentration of 0.05% w of catalyst presents a decrease in FAME production, which can be attributed to reaction equilibrium (Habaki *et al*., 2018). Moreover, in a three-phase system (oil-methanol-catalyst), a higher dose of catalyst tends to lead to the higher viscosity of the mixture resulting in mass transfer limitations of the reactants to reach the catalytic sites (Rocha *et al*., 2019). On the other hand, increasing the reaction time within certain limits increases the biodiesel yield. However, upon reaching 30 min of reaction, the formation of methyl esters decreases. The studied residues were predicted by the best fit of the normal distribution and were plotted against the studied residues obtained from experiments, as shown in Figure 9. It can be seen that the studied residues follow a normal distribution, as evidence from the straight line in Figure 9. The residues studied were plotted against the predicted biodiesel yield and data points are scattered randomly, indicating that values from original observations are not related to values of the response. Therefore, it can be deduced that the quadratic regression model gives an adequate description of the biodiesel production process.

The reuse of a catalyst is very important for its point of view of commercial viability. To test the reuse capacity of the CAS catalyst, it was repeatedly used for the conversion of oleic acid. After completion of the esterification reaction, the CAS catalyst was filtered and recovered from the mixture, washed with acetone to remove the glycerine and some adsorbed materials onto the surface, subsequently dried before reusing for

a longer reaction cycle in optimal conditions (Chhabra *et al*., 2018). It was found that the catalyst reusability could be sustained and after four cycles (Figure 10.). This proves that the catalyst is highly active and reusable for biodiesel production (Sangar *et al*., 2019).

Conclusions

The heterogeneous solid acid catalyst used in this work showed good performance in the production of fatty acid methyl esters and easy to be separated from the liquid mixture. The CAS catalyst consists of particles in different sizes and irregular diameters of 3-40 μm. In addition, the Raman, XRD, and ICTAC analysis confirmed that the catalyst exhibited an adequate stable sulfonyl group and thermal stability. This further confirms the effect of CAS improves the reaction rate by favorable interaction of oleic acid. With the aid of the response surface methodology based on the Box-Behnken design was successfully applied to study the effects of parameters during biodiesel production from oleic acid with methanol and sulfonated carbon as a catalyst. The highest percentage of conversion to biodiesel was 97.9 % yield. This performance was achieved under the optimum reaction conditions at 200 °C, a reaction time of 20 min and a catalyst amount of 0.03 wt.%. The conditions optimized to obtain the maximum performance with a design of experiments are the following: temperature of 198.1 °C, the catalyst load of 0.0346 wt% and a reaction time of 23.5 minutes. The maximum yield biodiesel in such conditions was 98.94%. Interestingly, easily recovered by filtration of CAS showed the constant stable catalytic conversion of biodiesel even after four consecutive cycles without regeneration. According to the ANOVA results, the catalyst concentration was the most significant factor among the other parameters as examined.

Nomenclature

CAS	Sulfonated Carbon
CTE	Carbonaceous Material
FAME	Fatty Acid Methyl Ester
FFA	Free Fatty Acids
W	Catalyst
T	Temperature
M	Reaction Time

References

Araujo, R. O., Chaar, J. da S., Queiroz, L. S., da Rocha Filho, G. N., da Costa, C. E. F., da Silva, G. C. T., Landers, R., Costa, M. J. F., Gonçalves, A. A. S., de Souza, L. K. C. (2019). Low temperature sulfonation of acai stone biomass derived carbons as acid catalysts for esterification reactions. *Energy Conversion and Management 196*, 821-830. https://doi.org/10.1016/j.enconman.2019.06.059

Atadashi, I. M., Aroua, M. K., Abdul Aziz, A. R., & Sulaiman, N. M. N. (2012). Production of biodiesel using high free fatty acid feedstocks. *Renewable and Sustainable Energy Reviews 16*, 3275-3285. https://doi.org/10.1016/j.rser.2012.02.063

Baharudin, K. B., Taufiq-Yap, Y. H., Hunns, J., Isaacs, M., Wilson, K., & Derawi, D. (2019). Mesoporous NiO/Al-SBA-15 catalysts for solvent-free deoxygenation of palm fatty acid distillate. *Microporous and Mesoporous Materials 276*, 13-22. https://doi.org/10.1016/j.micromeso.2018.09.014

Bing, W., & Wei, M. (2019). Recent advances for solid basic catalysts: Structure design and catalytic performance. *Journal of Solid State Chemistry 269*, 184-194. https://doi.org/10.1016/j.jssc.2018.09.023

Cannilla, C., Bonura, G., Costa, F., & Frusteri, F. (2018). Biofuels production by esterification of oleic acid with ethanol using a membrane assisted reactor in vapour permeation configuration. *Applied Catalysis A: General 566*, 121-129. https://doi.org/10.1016/j.apcata.2018.08.014

Cea, M., González, M. E., Abarzúa, M., & Navia, R. (2019). Enzymatic esterification of oleic acid by Candida rugosa lipase immobilized onto biochar. *Journal of Environmental Management 242*, 171-177. https://doi.org/10.1016/j.jenvman.2019.04.013

Chaveanghong, S., Smith, S. M., Smith, C. B., Luengnaruemitchai, A., & Boonyuen, S. (2018). Simultaneous transesterification and esterification of acidic oil feedstocks catalyzed by heterogeneous tungsten loaded bovine bone

under mild conditions. *Renewable Energy 126*, 156-162. https://doi.org/10.1016/j.renene.2018.03.036

Chellappan, S., Nair, V., Sajith, V., & Aparna, K. (2018). Synthesis, optimization and characterization of biochar based catalyst from sawdust for simultaneous esterification and transesterification. *Chinese Journal of Chemical Engineering 26*, 2654-2663. https://doi.org/10.1016/j.cjche.2018.02.034

Cheryl-Low, Y. L., Theam, K. L., & Lee, H. V. (2015). Alginate-derived solid acid catalyst for esterification of low-cost palm fatty acid distillate. *Energy Conversion and Management 106*, 932-940. https://doi.org/10.1016/j.enconman.2015.10.018

Chhabra, P., Zhou, L., Karimi, I. A., & Kraft, M. (2018). Exploiting meta-modeling approach to investigate the effect of oil characteristics on the optimal operating conditions and biodiesel properties. *Computer Aided Chemical Engineering 43*, 157-162. https://doi.org/10.1016/B978-0-444-64235-6.50029-2

Choi, D., Yoo, S. H., & Lee, S. (2019). Safer and more effective route for polyethylene-derived carbon fiber fabrication using electron beam irradiation. *Carbon 146*, 9-16. https://doi.org/10.1016/j.carbon.2019.01.061

Dejean, A., Ouédraogo, I. W. K., Mouras, S., Valette, J., & Blin, J. (2017). Shea nut shell based catalysts for the production of ethanolic biodiesel. *Energy for Sustainable Development 40*, 103-111. https://doi.org/10.1016/j.esd.2017.07.006

Dhawane, S. H., Kumar, T., & Halder, G. (2016). Biodiesel synthesis from Hevea brasiliensis oil employing carbon supported heterogeneous catalyst: Optimization by Taguchi method. *Renewable Energy 89*, 506-514. https://doi.org/10.1016/j.renene.2015.12.027

Dhawane, S. H., Kumar, T., & Halder, G. (2018). Recent advancement and prospective of heterogeneous carbonaceous catalysts in chemical and enzymatic transformation of biodiesel. *Energy Conversion and Management 167*, 176-202. https://doi.org/10.1016/j.enconman.2018.04.073

Douzandegi Fard, M. A., Ghafuri, H., & Rashidizadeh, A. (2019). Sulfonated highly ordered mesoporous graphitic carbon nitride as a super active heterogeneous solid acid catalyst for Biginelli reaction. *Microporous and Mesoporous Materials 274*, 83-93. https://doi.org/10.1016/j.micromeso.2018.07.030

Efimov, M. N., Sosenkin, V. E., Volfkovich, Y. M., Vasilev, A. A., Muratov, D. G., Baskakov, S. A., Efimov, O. N., & Karpacheva, G. P. (2018). Electrochemical performance of polyacrylonitrile-derived activated carbon prepared via IR pyrolysis. *Electrochemistry Communications 96*, 98-102. https://doi.org/10.1016/j.elecom.2018.10.016

Fadhil, A. B., Aziz, A. M., & Al-Tamer, M. H. (2016). Biodiesel production from Silybum marianum L. seed oil with high FFA content using sulfonated carbon catalyst for esterification and base catalyst for transesterification. *Energy Conversion and Management 108*, 255-265. https://doi.org/10.1016/j.enconman.2015.11.013

Farobie, O., & Matsumura, Y. (2017). Continuous production of biodiesel under supercritical methyl acetate conditions: Experimental investigation and kinetic model. *Bioresource Technology 241*, 720-725. https://doi.org/10.1016/j.biortech.2017.05.210

Ferreira, A. R. O., Silvestre-Albero, J., Maier, M. E., Ricardo, N. M. P. S., Cavalcante, C. L., & Luna, F. M. T. (2020). Sulfonated activated carbons as potential catalysts for biolubricant synthesis. *Molecular Catalysis 488*, 110888. https://doi.org/10.1016/j.mcat.2020.110888

Fraile, J. M., García-Bordejé, E., Pires, E., & Roldán, L. (2015). Catalytic performance and deactivation of sulfonated hydrothermal carbon in the esterification of fatty acids: Comparison with sulfonic solids of different nature. *Journal of Catalysis 324*, 107-118. https://doi.org/10.1016/j.jcat.2014.12.032

Gao, Z., Tang, S., Cui, X., Tian, S., & Zhang, M. (2015). Efficient mesoporous carbon-based solid catalyst for the esterification of oleic acid. *Fuel 140*, 669-676. https://doi.org/10.1016/j.fuel.2014.10.012

Guan, Q., Li, Y., Chen, Y., Shi, Y., Gu, J., Li, B., Miao, R., Chen, Q., & Ning, P. (2017). Sulfonated multi-walled carbon nanotubes for biodiesel production through triglycerides transesterification. *RSC Advances 12*. https://doi.org/10.1039/c6ra28067f

Habaki, H., Hayashi, T., & Egashira, R. (2018). Deacidification process of crude inedible plant oil by esterification for biodiesel production. *Journal of Environmental Chemical Engineering 6*, 3054-3060. https://doi.org/10.1016/j.jece.2018.04.039

Hajamini, Z., Sobati, M. A., Shahhosseini, S., & Ghobadian, B. (2016). Waste fish oil (WFO) esterification catalyzed by sulfonated activated carbon under ultrasound irradiation. *Applied Thermal Engineering 94*, 141-150. https://doi.org/10.1016/j.applthermaleng.2015.10.101

Hood, Z. D., Adhikari, S. P., Li, Y., Naskar, A. K., Figueroa-Cosme, L., Xia, Y., Chi, M., Wright, M. W., Lachgar, A., & Paranthaman, M. P. (2017). Novel acid catalysts from waste-tire-derived carbon: Application in waste-to-biofuel conversion. *ChemistrySelect 2*, 4975-4982. https://doi.org/10.1002/slct.201700869

Hood, Z. D., Adhikari, S. P., Evans, S. F., Wang, H., Li, Y., Naskar, A. K., Chi, M., Lachgar, A., & Paranthaman, M. P. (2018). Tire-derived carbon for catalytic preparation of biofuels from feedstocks containing free fatty acids. *Carbon Resources Conversion 1*, 165-173. https://doi.org/10.1016/j.crcon.2018.07.007 Hood, Z. D., Cheng, Y., Evans, S. F., Adhikari, S. P., & Parans Paranthaman, M. (2019). Unraveling the structural properties and dynamics of sulfonated solid acid carbon catalysts with neutron vibrational spectroscopy. *Catalysis Today (October)*. https://doi.org/10.1016/j.cattod.2019.10.033

Hosseini, M. S., Masteri-Farahani, M., & Shahsavarifar, S. (2019). Chemical modification of reduced graphene oxide with sulfonic acid groups: Efficient solid acids for acetalization and esterification reactions. *Journal of the Taiwan Institute of Chemical Engineers 102*, 34-43. https://doi.org/10.1016/j.jtice.2019.05.020

Hosseini, S., Janaun, J., & Choong, T. S. Y. (2015). Feasibility of honeycomb monolith supported sugar catalyst to produce biodiesel from palm fatty acid distillate (PFAD). *Process Safety and Environmental Protection 98*, 285-295. https://doi.org/10.1016/j.psep.2015.08.011

Jia, M., Jiang, L., Niu, F., Zhang, Y., & Sun, X. (2018). A novel and highly efficient esterification process using triphenylphosphine oxide with oxalyl chloride. *Royal Society Open Science 5*. https://doi.org/10.1098/rsos.171988

Jiang, Y., Lu, J., Sun, K., Ma, L., & Ding, J. (2013). Esterification of oleic acid with ethanol catalyzed by sulfonated cation exchange resin: Experimental and kinetic studies. *Energy Conversion and Management 76*, 980-985. https://doi.org/10.1016/j.enconman.2013.08.011

Kumar, V., Muthuraj, M., Palabhanvi, B., Ghoshal, A. K., & Das, D. (2014). Evaluation and optimization of two stage sequential in situ transesterification process for fatty acid methyl ester quantification from microalgae. *Renewable Energy 68*, 560-569. https://doi.org/10.1016/j.renene.2014.02.037

Kurniawan, J., Suga, K., & Kuhl, T. L. (2017). Interaction forces and membrane charge tunability: Oleic acid containing membranes in different pH conditions. *Biochimica et Biophysica Acta - Biomembranes 1859*, 211-217. https://doi.org/10.1016/j.bbamem.2016.11.001

Latchubugata, C. S., Kondapaneni, R. V., Patluri, K. K., Virendra, U., & Vedantam, S. (2018). Kinetics and optimization studies using Response Surface Methodology in biodiesel production using heterogeneous catalyst. *Chemical Engineering Research and Design 135*, 129-139. https://doi.org/10.1016/j.cherd.2018.05.022

Li, N., Wang, Q., Ullah, S., Zheng, X. C., Peng, Z. K., & Zheng, G. P. (2019). Esterification of levulinic acid in the production of fuel additives catalyzed by porous sulfonated carbon derived from pine needle. *Catalysis Communications 129*, 105755. https://doi.org/10.1016/j.catcom.2019.105755

Liu, L., Wen, Z., & Cui, G. (2015). Preparation of Ca/Zr mixed oxide catalysts through a birch-templating route for the synthesis of biodiesel via transesterification. *Fuel 158*, 176-182. https://doi.org/10.1016/j.fuel.2015.05.025

Lokman, I. M., Rashid, U., & Taufiq-Yap, Y. H. (2016). Meso- and macroporous sulfonated starch solid acid catalyst for esterification of palm fatty acid distillate. *Arabian Journal of Chemistry 9*, 179-189. https://doi.org/10.1016/j.arabjc.2015.06.034

Long, Y. D., Fang, Z., Su, T. C., & Yang, Q. (2014). Co-production of biodiesel and hydrogen from rapeseed and Jatropha oils with sodium silicate and Ni catalysts. *Applied Energy 113*, 1819-1825. https://doi.org/10.1016/j.apenergy.2012.12.076

Lozano, P., Bernal, J. M., Sánchez-Gómez, G., López-López, G., & Vaultier, M. (2013). How to produce biodiesel easily using a green biocatalytic approach in sponge-like ionic liquids. *Energy and Environmental Science 4*. https://doi.org/10.1039/c3ee24429f

Medina-Valtierra, J., Sánchez-Olmos, L. A., Carrasco-Marin, F., & Sánchez-Cárdenas, M. (2017). Optimization models type box-behnken in the obtaining of biodiesel from waste frying oil using a large-acidity carbonaceous catalyst. *International Journal of Chemical Reactor Engineering 15*. https://doi.org/10.1515/ijcre-2017-0072

Mohammed, N. I., Kabbashi, N. A., Alam, M. Z., & Mirghani, M. E. S. (2016). Esterification of Jatropha curcas hydrolysate using powdered niobic acid catalyst. JournaloftheTaiwanInstituteofChemicalEngineers63, 243-249. https://doi.org/10.1016/j.jtice.2016.03.007

Mota, F. A. S., Costa Filho, J. T., & Barreto, G. A. (2019). The Nile tilapia viscera oil extraction for biodiesel production in Brazil: An economic analysis. *Renewable and Sustainable Energy Reviews 108*, 1-10. https://doi.org/10.1016/j.rser.2019.03.035

Ning, Y., & Niu, S. (2017). Preparation and catalytic performance in esterification of a bamboo-based heterogeneous acid catalyst with microwave assistance. *Energy Conversion and Management 153*, 446-454. https://doi.org/10.1016/j.enconman.2017.10.025

Noshadi, I., Kanjilal, B., Du, S., Bollas, G. M., Suib, S. L., Provatas, A., Liu, F., & Parnas, R. S. (2014). Catalyzed production of biodiesel and bio-chemicals from brown grease using ionic liquid functionalized ordered mesoporous polymer. *Applied Energy 129*, 112-122. https://doi.org/10.1016/j.apenergy.2014.04.090 Paysepar, H., Tirumala, K., Rao, V., Yuan, Z., & Nazari, L. (2018). Zeolite catalysts screening for production of phenolic bio-oils with high contents of monomeric aromatics / phenolics from hydrolysis lignin via catalytic fast pyrolysis. *Fuel Processing Technology (April)*. https://doi.org/10.1016/j.fuproc.2018.07.013

Pisarello, M. L., Maquirriain, M., Sacripanti Olalla, P., Rossi, V., & Querini, C. A. (2018). Biodiesel production by transesterification in two steps: Kinetic effect or shift in the equilibrium conversion. *Fuel Processing Technology*. https://doi.org/10.1016/j.fuproc.2018.09.028

Purova, R., Narasimharao, K., Ahmed, N. S. I., Al-Thabaiti, S., Al-Shehri, A., Mokhtar, M., & Schwieger, W. (2015). Pillared HMCM-36 zeolite catalyst for biodiesel production by esterification of palmitic acid. *Journal of Molecular Catalysis A: Chemical 406*, 159-167. https://doi.org/10.1016/j.molcata.2015.06.006

Rechnia-Goracy, P., Malaika, A., & Kozłowski, M. (2019). Effective conversion of rapeseed oil to biodiesel fuel in the presence of basic activated carbon catalysts. *Catalysis Today*. https://doi.org/10.1016/j.cattod.2019.05.055

Rocha, J. G., Mendonça, A. D. M., de Campos, D. A. R., Mapele, R. O., Barra, C. M., Bauerfeldt, G. F., & Tubino, M. (2019). Biodiesel synthesis: Influence of alkaline catalysts in methanol-oil dispersion. *Journal of the Brazilian Chemical Society 30*, 342-349. https://doi.org/10.21577/0103-5053.20180183

Sánchez-Cárdenas, M., Medina-Valtierra, J., Kamaraj, S. K., Trejo-Zárraga, F., & Antonio

Sánchez-Olmos, L. (2017). Physicochemical effect of Pt nanoparticles/γ-Al_2O_3 on the oleic acid hydrodeoxygenation to biofuel. *Environmental Progress and Sustainable Energy 36*, 1224-1233. https://doi.org/10.1002/ep.12563

Sánchez-Cárdenas, M., Medina-Valtierra, J., Kamaraj, S.-K., Medina Ramírez, R., & Sánchez-Olmos, L. (2016). Effect of size and distribution of Ni nanoparticles on γ-Al_2O_3 in oleic acid hydrodeoxygenation to produce n-alkanes. *Catalysts 6*, 156. https://doi.org/10.3390/catal6100156

Sánchez-Olmos, L. A., Medina-Valtierra, J., Sathish-Kumar, K., & Sánchez Cardenas, M. (2017). Sulfonated char from waste tire rubber used as strong acid catalyst for biodiesel production. *Environmental Progress and Sustainable Energy 36*, 619-626. https://doi.org/10.1002/ep.12499

Sánchez-Olmos, L. A., Sánchez-Cárdenas, M., Sathish-Kumar, K., Tirado-González, D. N., Maldonado-Ruelas, V. A., & Ortiz-Medina, R. A. (2019). Effect of the sulfonated catalyst in obtaining biodiesel when used in a diesel engine with controlled tests. *Revista Mexicana de Ingeniería Química 19*, 969-982. https://doi.org/10.24275/rmiq/ie831

Sangar, S. K., Syazwani, O. N., Farabi, M. S. A., Razali, S. M., Shobhana, G., Teo, S. H., & Taufiq-Yap, Y. H. (2019). Effective biodiesel synthesis from palm fatty acid distillate (PFAD)using carbon-based solid acid catalyst derived glycerol. *Renewable Energy 142*, 658-667. https://doi.org/10.1016/j.renene.2019.04.118

Santos, E. M., Teixeira, A. P. D. C., Da Silva, F. G., Cibaka, T. E., Araújo, M. H., Oliveira, W. X. C., Medeiros, F., Brasil, A. N., De Oliveira, L. S., & Lago, R. M. (2015). New heterogeneous catalyst for the esterification of fatty acid produced by surface aromatization/sulfonation of oilseed cake. *Fuel 150*, 408-414. https://doi.org/10.1016/j.fuel.2015.02.027

Saravanan, K., Tyagi, B., & Bajaj, H. C. (2016). Nano-crystalline, mesoporous aerogel sulfated zirconia as an efficient catalyst for esterification of stearic acid with methanol. *Applied Catalysis B: Environmental 192*, 161-170. https://doi.org/10.1016/j.apcatb.2016.03.037

Saravanan, K., Tyagi, B., Shukla, R. S., & Bajaj, H. C. (2015). Esterification of palmitic acid with methanol over template-assisted mesoporous sulfated zirconia solid acid catalyst. *Applied Catalysis B: Environmental 172-173*, 108-115. https://doi.org/10.1016/j.apcatb.2015.02.014

Sarno, M., & Iuliano, M. (2018). Active biocatalyst for biodiesel production from spent coffee ground. *Bioresource Technology 266*, 431-438. https://doi.org/10.1016/j.biortech.2018.06.108

Shi, Y., & Liang, X. (2019). Novel carbon microtube based solid acid from pampas grass stick for biodiesel synthesis from waste oils. *Journal of Saudi Chemical Society 23*, 515-524. https://doi.org/10.1016/j.jscs.2018.09.004

Shukla, A., Bhat, S. D., & Pillai, V. K. (2016). Simultaneous unzipping and sulfonation of multi-walled carbon nanotubes to sulfonated graphene nanoribbons for nanocomposite membranes in polymer electrolyte fuel cells. *Journal of Membrane Science 520*, 657-670. https://doi.org/10.1016/j.memsci.2016.08.019

Singh, S., & Patel, A. (2017). Value added products derived from biodiesel waste glycerol: activity, selectivity, kinetic and thermodynamic evaluation over anchored lacunary phosphotungstates. *Journal of Porous Materials 24*, 1409-1423. https://doi.org/10.1007/s10934-017-0382-5

Sirisomboonchai, S., Abuduwayiti, M., Guan, G., Samart, C., Abliz, S., Hao, X., Kusakabe, K., & Abudula, A. (2015). Biodiesel production from waste cooking oil using calcined scallop shell as catalyst. *Energy Conversion and Management 95*, 242-247. https://doi.org/10.1016/j.enconman.2015.02.044

Tang, J., Yu, C., Wang, R., & Liu, J. (2019). Sulfonation of graphene and its effects on tricalcium silicate hydration. *Construction and Building Materials 206*, 600-608. https://doi.org/10.1016/j.conbuildmat.2019.01.155

Teo, S. H., Islam, A., Yusaf, T., & Taufiq-Yap, Y. H. (2014). Transesterification of Nannochloropsis oculata microalga's oil to biodiesel using calcium methoxide catalyst. *Energy 78*, 63-71. https://doi.org/10.1016/j.energy.2014.07.045 Veiga, P. M., Gomes, A. C. L., Veloso, C. O., & Henriques, C. A. (2017). Acid zeolites for glycerol etherification with ethyl alcohol: Catalytic activity and catalyst properties. *Applied Catalysis A: General 548*, 2-15. https://doi.org/10.1016/j.apcata.2017.06.042

Veljković, V. B., Veličković, A. V., Avramović, J. M., & Stamenković, O. S. (2018). Modeling of biodiesel production: Performance comparison of Box-Behnken, face central composite and full factorial design. *Chinese Journal of Chemical Engineering 27*, 1690-1698. https://doi.org/10.1016/j.cjche.2018.08.002

Wang, Y., Wang, X., Xie, Y., & Zhang, K. (2018). Functional nanomaterials through esterification of cellulose: a review of chemistry and application. *Cellulose 25*, 3703-3731. https://doi.org/10.1007/s10570-018-1830-3

Xie, W., & Zhao, L. (2014). Heterogeneous CaO-MoO_3-SBA-15 catalysts for biodiesel production from soybean oil. *Energy Conversion and Management 79*, 34-42. https://doi.org/10.1016/j.enconman.2013.11.041

Yuvaraj, P., Rao, J. R., Fathima, N. N., Natchimuthu, N., & Mohan, R. (2018). Complete replacement of carbon black filler in rubber sole with CaO embedded activated carbon derived from tannery solid waste. *Journal of Cleaner Production 170*, 446-450. https://doi.org/10.1016/j.jclepro.2017.09.188

Zhang, D. Y., Duan, M. H., Yao, X. H., Fu, Y. J., & Zu, Y. G. (2016). Preparation of a novel cellulose-based immobilized heteropoly acid system and its application on the biodiesel production. *Fuel 172*, 293-300. https://doi.org/10.1016/j.fuel.2015.12.020

Zhang, H., Li, H., Pan, H., Wang, A., Souzanchi, S., Xu, C. (Charles), & Yang, S. (2018). Magnetically recyclable acidic polymeric ionic liquids decorated with hydrophobic regulators as highly efficient and stable catalysts for biodiesel production. *Applied Energy 223*, 416-429. https://doi.org/10.1016/j.apenergy.2018.04.061

Zhou, Y., Niu, S., & Li, J. (2016). Activity of the carbon-based heterogeneous acid catalyst derived from bamboo in esterification of oleic acid with ethanol. *Energy Conversion and Management 114*, 188-196. https://doi.org/10.1016/j.enconman.2016.02.027

Zhou, Y., Schideman, L., Yu, G., & Zhang, Y. (2013). A synergistic combination of algal wastewater treatment and hydrothermal biofuel production maximized by nutrient and carbon recycling. *Energy and Environmental Science 12*. https://doi.org/10.1039/C3EE24241B